The 2015 World Congress on
Advances in Civil, Environmental, and Materials Research (ACEM15)
Incheon, Korea, August 25-29, 2015

Dynamic Characteristics of Thin-Walled Composite Beams Subjected to Electromagnetic and Thermal Fields

* Sang-Yun Park[1] and Ohseop Song[2]

[1], [2] *Department of Mechanical Engineering, Chungnam National University, Daejeon 305-764, Republic of Korea*
[2] songos@cnu.ac.kr

ABSTRACT

Structural model of a laminated composite thin-walled beam subjected to a combination of electromagnetic and thermal fields is developed. Coupled equations motion are derived via Hamilton's principle on the basis of electromagnetic equations and thermal equations which are involved in constitutive equations. Extended Galerkin method is adopted to obtain discretized equations of motion. Variations of dynamic characteristics of composite thin-walled beams with applied electromagnetic field, temperature gradient and ply angle for a cantilever boundary condition are investigated and pertinent conclusions are derived.

1. INTRODUCTION

The multi-functional structures subjected to interactive elastic, thermal, magnetic and electric fields is likely to bring a new dimension to the design of smart structures. The multi-functional structures may find their applications in the fields of the aerospace industry, nuclear power plants, magnetic suspension systems, and electromechanical devices such as micro-actuators. A better understanding of their static and dynamic behavior when subjected to fully interactive actions is necessary. Multiple properties of materials/structures are exploited in such a way that besides its major structural function, the same structural component may accomplish at least one more task.

The dynamic behavior of a system subjected to a combined electromagnetic-thermal field constitutes one of the most interesting fields of study for researchers (Kim et al., 2011; Moon, 1984). The coupling between electromagnetic-thermal-elasticity for different stacking sequences of laminated composite structures should be considered in the design of such structures and systems. (Qin and Hasanyan 2011) and (Qin 2010) carried out pioneering research work on the nonlinear responses and stability of isotropic/composite cylindrical shells. (Tsai and Wu 2008) performed a free vibration analysis of a functionally graded magnetic-electric-elastic shell with an open-circuit surface condition. (Yoon 2010) performed the topology optimization that considered the electro-fluid-thermal-compliant couplings for a micro-actuator.

---

[1] Graduate Student
[2] Professor

2. EQUATIONS OF MOTION

2.1 Displacement field

Two coordinate systems are used in the forthcoming development:

Fig. 1 shows the geometry and coordinates of composite thin-walled beam. (X,Y,Z) denotes the global coordinate system while (n,s,z) is local coordinate system. X and Y are global cross-section coordinates and Z is axial coordinate. (n, s) denote thickness coordinate normal to the beam mid-surface and tangential coordinate along the contour line of the beam cross-section, respectively.

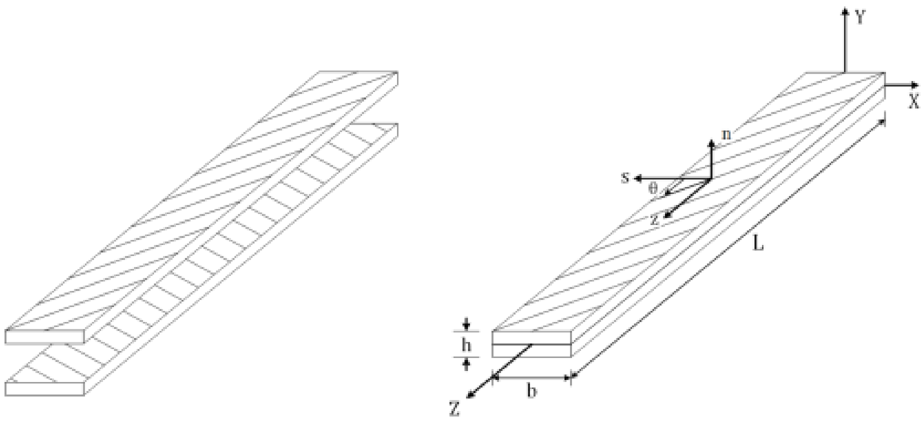

Fig. 1 Configurations of composite thin-walled I- beam and box beam

In order to reduce the 3-D elasticity problem to an equivalent 1-D one, the components of the 3-D displacement vector are expressed as: (Thin-Walled Composite beams,2006)

$$u(x,y,z,t) = u_0(z,t) - y\emptyset(z,t) \quad (1a)$$

$$v(x,y,z,t) = v_0(z,t) + x\emptyset(z,t) \quad (1b)$$

$$w(x,y,z,t) = w_0(z,t) + \theta_x(z,t)\left[y(s) - n\frac{dx}{ds}\right] + \theta_y(z,t)\left[x(s) + n\frac{dy}{ds}\right] - \emptyset'(z,t)[F_w(s) - nr_t(s)] \quad (1c)$$

where $u_0(z,t), v_0(z,t), w_0(z,t)$ are denote the rigid body translations along the x-, y- and z-axes, while $\theta_x(z,t)$, $\theta_y(z,t)$ and $\emptyset(z,t)$ denote the rigid body rotations about the x- and y-axes and the twist about the z-axis, respectively

2.2 Electromagnetic field and thermal field equations

The electromagnetic equations are derived from the generalized Maxwell equations as Kim (2011)

$$\text{Ohm's law} \qquad \mathbf{J} = G(\mathbf{E} + \dot{\mathbf{U}} \times \mathbf{B}) \quad (2a)$$

$$\text{Lorentz force} \qquad \mathbf{f} = \mathbf{J} \times \mathbf{B} \quad (2b)$$

where **E** denotes the electric field vector, **J** is the current density vector, and **B** is the magnetic induction intensity vector. **f** is the Lorentz force vector per unit volume.

Matrix **G** represents the electric conductivity matrix of a composite beam.

$$G \equiv \begin{bmatrix} g_{11} & g_{12} & 0 \\ g_{12} & g_{22} & 0 \\ 0 & 0 & g_{33} \end{bmatrix} \tag{3}$$

Electric field, displacement vector and magnetic field vector are expressed as:

$$\mathbf{E} = E_{01}^0 \mathbf{i_1} + E_{02}^0 \mathbf{i_2} + E_{03}^0 \mathbf{i_3} \tag{4b}$$
$$\dot{\mathbf{U}} = (\dot{u}_0\text{-}y\dot{\emptyset})\mathbf{i_1} + (\dot{v}_0 + x\dot{\emptyset})\mathbf{i_2} + (\dot{w}_0 + \dot{\theta}_x y + \dot{\theta}_y x\text{-}F_w\dot{\emptyset}')\,\mathbf{i_3} \tag{4a}$$
$$\mathbf{B} = (B_{01}^0 + \mathbf{z}B_{01}^0)\mathbf{i_1} + (B_{02}^0 + \mathbf{z}B_{02}^1)\mathbf{i_2} + (B_{03}^0 + \mathbf{z}B_{03}^1)\mathbf{i_3} \tag{4c}$$

$$\dot{\mathbf{U}} \times \mathbf{B} = \begin{vmatrix} \mathbf{i_1} & \mathbf{i_2} & \mathbf{i_3} \\ \dot{u}_0 - y\dot{\emptyset} & \dot{v}_0 + x\dot{\emptyset} & \dot{w}_0 + \dot{\theta}_x y + \dot{\theta}_y x - F_w\dot{\emptyset}' \\ (B_{01}^0 + \mathbf{z}B_{02}^0) & (B_{02}^0 + \mathbf{z}B_{02}^1) & (B_{03}^0 + \mathbf{z}B_{03}^1) \end{vmatrix} \tag{5}$$
$$= [(\dot{v}_0 + x\dot{\emptyset})\,(B_{03}^0 + \mathbf{z}B_{03}^1) - (B_{02}^0 + \mathbf{z}B_{02}^1)(\dot{w}_0 + \dot{\theta}_x y + \dot{\theta}_y x - F_w\dot{\emptyset}')]\,\mathbf{i_1}$$
$$-[(\dot{u}_0 - y\dot{\emptyset})\,(B_{03}^0 + \mathbf{z}B_{03}^1) - (B_{01}^0 + \mathbf{z}B_{02}^0)(\dot{w}_0 + \dot{\theta}_x y + \dot{\theta}_y x - F_w\dot{\emptyset}')]\,\mathbf{i_2}$$
$$+[(\dot{u}_0 - y\dot{\emptyset})\,(B_{02}^0 + \mathbf{z}B_{02}^1) - (B_{01}^0 + \mathbf{z}B_{01}^0)(\dot{v}_0 + x\dot{\emptyset})]\,\mathbf{i_3}$$

Ohm's law is obtained by substituting Eq.(4) into Eq.(2a)

$$\mathbf{J} = G(\mathbf{E} + \dot{\mathbf{U}} \times \mathbf{B}) = \mathbf{J_1}\mathbf{i_1} + \mathbf{J_2}\mathbf{i_2} + \mathbf{J_3}\mathbf{i_3} \tag{6}$$

Lorentz force vector is obtained by substituting Eq.(6) and Eq.(4c) into Eq.(2b) as

$$\mathbf{f} = \mathbf{J} \times \mathbf{B} = (J_1\mathbf{i_1} + J_2\mathbf{i_2} + J_3\mathbf{i_3}) \times ((B_{01}^0 + \mathbf{z}B_{02}^0)\mathbf{i_1} + (B_{02}^0 + \mathbf{z}B_{02}^1)\mathbf{i_2} + (B_{03}^0 + \mathbf{z}B_{03}^1)\mathbf{i_3})$$
$$= \begin{vmatrix} \mathbf{i_1} & \mathbf{i_2} & \mathbf{i_3} \\ J_1 & J_2 & J_3 \\ (B_{01}^0 + \mathbf{z}B_{01}^0) & (B_{02}^0 + \mathbf{z}B_{02}^1) & (B_{03}^0 + \mathbf{z}B_{03}^1) \end{vmatrix}$$

It is assumed that only the electric field in the axial direction B_{03}^0 is applied and the magnetic field in thickness direction E_{02}^0 exists.
Therefore, Lorentz force is reduced to the following form as

$$\mathbf{f_1} = \boldsymbol{g}_{\mathbf{12}}^{(i)}(\dot{v}_0 B_{03}^0 + \mathbf{x}\dot{\emptyset}B_{03}^0) + \boldsymbol{g}_{\mathbf{22}}^{(i)}(E_{02}^0 B_{03}^0 - \dot{u}_0 B_{03}^0 + y\dot{\emptyset}B_{03}^0) \tag{7a}$$
$$\mathbf{f_2} = -\boldsymbol{g}_{\mathbf{11}}^{(i)}(\dot{v}_0 B_{03}^0 + \mathbf{x}\dot{\emptyset}B_{03}^0) + \boldsymbol{g}_{\mathbf{12}}^{(i)}(E_{02}^0 B_{03}^0 - \dot{u}_0 B_{03}^0 + y\dot{\emptyset}B_{03}^0) \tag{7b}$$
$$\mathbf{f_3} = \mathbf{0} \tag{7c}$$

Thermal stress resultants caused from temperature gradient are expressed as

$$\mathbf{N_1^T} = \Delta\mathbf{T}\sum_{\mathbf{k=1}}^{\mathbf{N}} [\overline{\mathbf{Q_{11}}}\,\boldsymbol{\alpha_s} + \overline{\mathbf{Q_{12}}}\boldsymbol{\alpha_z} + \overline{\mathbf{Q_{13}}}\boldsymbol{\alpha_n} + \overline{\mathbf{Q_{16}}}\boldsymbol{\alpha_{sz}}]_{(k)}(\boldsymbol{n_{(k)}} - \boldsymbol{n_{(k-1)}}) \tag{8a}$$

$$\mathbf{N_2^T} = \Delta\mathbf{T}\sum_{\mathbf{k=1}}^{\mathbf{N}}[\overline{\mathbf{Q_{16}}}\,\boldsymbol{\alpha_s} + \overline{\mathbf{Q_{26}}}\boldsymbol{\alpha_z} + \overline{\mathbf{Q_{36}}}\boldsymbol{\alpha_n} + \overline{\mathbf{Q_{66}}}\boldsymbol{\alpha_{sz}}]_{(k)}\left(\boldsymbol{n_{(k)}} - \boldsymbol{n_{(k-1)}}\right) \tag{8b}$$

$$\mathbf{N_4^T} = \Delta\mathbf{T}\sum_{\mathbf{k=1}}^{\mathbf{N}}[\overline{\mathbf{Q_{12}}}\,\boldsymbol{\alpha_s} + \overline{\mathbf{Q_{22}}}\boldsymbol{\alpha_z} + \overline{\mathbf{Q_{23}}}\boldsymbol{\alpha_n} + \overline{\mathbf{Q_{26}}}\boldsymbol{\alpha_{sz}}]_{(k)}\left(\boldsymbol{n^2_{(k)}} - \boldsymbol{n^2_{(k-1)}}\right) \tag{8c}$$

2.3 Equation of motion and boundary condition

The virtual work principle is used to derive the equations of equilibrium and associated boundary conditions. Where δ is the first variation operator, T is the kinetic energy, U is the potential energy, and W_e is the work done by Lorentz force and thermal load.

$$\delta J = \delta\int_{t_0}^{t_1}[T - U + W_e]dt = 0 \tag{9}$$

when thermal loads and a magnetic field is applied in the axial direction into a thin beam and the electric field is applied in the thickness direction, motion equations and boundary conditions are as follows.

(1) Equations of motion:

$$\delta u_0: a_{43}\theta_x'' + a_{44}\left(u_0'' + \theta_y'\right) - b_1\ddot{u}_0 - B_{12}\dot{v}_0 + B_{22}\dot{u}_0 - E_1 = 0 \tag{10a}$$

$$\delta v_0: a_{52}\theta_y'' + a_{55}(v_0'' + \theta_x') - b_1\ddot{v}_0 + B_{11}\dot{v}_0 - B_{12}\dot{u}_0 - E_2 = 0 \tag{10b}$$

$$\delta\theta_y: a_{22}\theta_y'' - a_{44}\left(u_0' + \theta_y\right) - a_{43}\theta_x' - b_5\ddot{\theta}_y + h_4 = 0 \tag{10c}$$

$$\delta\theta_x: a_{33}\theta_x'' + a_{34}\left(u_0'' + \theta_y'\right) - a_{55}\left(v_0' + \theta_x\right) - (b_4 + b_{14})\ddot{\theta}_x = 0 \tag{10e}$$

(2) Boundary conditions:

at $x = 0$:

$$u_0 = v_0 = \theta_y = \theta_x = 0 \tag{11a}$$

at $z = L$:

$$a_{43}\theta_x' + a_{44}\left(u_0' + \theta_y\right) - h_4 = 0 \tag{11b}$$

$$a_{55}\left(v_0' + \theta_x\right) = 0 \tag{11c}$$

$$a_{22}\theta_y' = 0 \tag{11d}$$

$$a_{33}\theta_x' + a_{34}\left(u_0' + \theta_y\right) - h_3 = 0 \tag{11e}$$

3. THE DISCRETIZED GOVERING EQUATION OF THIN WALLED BEAM

The governing equations are discretized through the extended Galerkin method. The following trial functions are chosen to satisfy boundary conditions as many as possible.

$$\left(u_0(x;t), v_0(x;t), \theta_y(x;t), \theta_x(x;t)\right) = \left(U(z), V(z), Y(z), X(z)\right)e^{i\omega t} \quad (12a)$$

$$\left(U(z), V(z), Y(z), X(z)\right) = \sum_{j=1}^{N}\left(a_j u_j(z), b_j u_j(z), c_j u_j(z), d_j u_j(z)\right) \quad (12b)$$

Substitution of Eqs. (12) into the equations of motion in conjunction with the boundary conditions yields the following discretized equations of motion:

$$[M]\ddot{\mathbf{q}}(t) + [C]\dot{\mathbf{q}}(t) + [K]\mathbf{q}(t) = 0 \quad (13)$$

The above equations of motion are transformed into a state equation as follows:

$$[M]^*\dot{\mathbf{x}}(t) + [K]^*\mathbf{x}(t) = 0 \quad (14)$$

where $[M]^* = \begin{bmatrix} M & 0 \\ 0 & -K \end{bmatrix}, [K]^* = \begin{bmatrix} C & K \\ K & 0 \end{bmatrix}, \mathbf{x} = \begin{Bmatrix} \dot{\mathbf{q}} \\ \mathbf{q} \end{Bmatrix}$

Eq. (19) is transformed into an eigenvalue problem as:

$$\lambda[M]^*\mathbf{x} + [K]^{**}\mathbf{x} = 0 \quad (15)$$

where λ denotes complex eigenvalues, $\lambda_r = \sigma_r \pm i\omega_{dr}$, where σ_r is the modal damping ratio and ω_{dr} is the r-th damped natural frequency. $\mathbf{x}$ is a state vector which contains modal vectors.

4. NUMERICAL RESULTS AND DISCUSSION

Fig.2 shows the variation in the natural frequencies with fiber angle for different values of magnetic field B_{03}^0. As the magnetic field intensity B_{03}^0 increases, the natural frequency decreases because the applied magnetic field produces an extra damping. The natural frequency increases as the fiber angle increases and is maximized at 90deg. where the stiffness is maximum. The results is symmetrical with respect to fiber angle 90 deg.

Fig.3 represents the variation in the natural frequencies with B_{03}^0 for three different fiber angle cases. Magnetic field provides an additional damping on the structure and as a result natural frequencies are decreased. As can be seen in Fig. (2), natural frequency for a case of fiber angle 90 deg. is larger than other cases.

Fig.4 shows the variation in the natural frequencies with fiber angle for three different temperature gradients. It indicates that the temperature gradient changes the stiffness quantities of structure. Compared with a positive temperature gradient case, a negative temperature gradient increases the stiffness and as a result, the increase of the natural frequency is observed.

Fig.5 reveals the variation in the natural frequencies with B_{03}^0 for three different electric fields. As the magnetic field intensity B_{03}^0 increases, the natural frequency decreases as can be seen in Fig.(3). Electric field has an effect only when magnetic field is not zero. The effect of electric field exists in the form of product with a magnetic field as can be seen in

Eq. (7). It is also shown that smaller electric field requires a larger magnetic field to derive the natural frequency to zero.

Fig. 6 shows the variation in the natural frequencies with fiber angle for three different electric fields. As the fiber angle increases, the natural frequency increases as can be seen in Fig. (4). It also reveals that the larger the electric field is, the lower the natural frequencies are.

Fig. 7 shows the variation in the natural frequencies with fiber angle for different B_{03}^{0}. As the fiber angle increases, the natural frequency increases as can be seen in Fig. (4). As the magnetic field intensity B_{03}^{0} increases, the natural frequency decreases.
It is shown that the smaller the fiber angle is, the sensitivity of magnetic field to the change in the natural frequency is more prominent compared with larger fiber angle cases.

Fig. 8 reveals the variation in the natural frequencies with B_{03}^{0} for different fiber angles. It is shown that the increases of the magnetic field intensity B_{03}^{0} results in the decrease of the natural frequency as can be seen in Fig. (3). It is also shown that the rate of change of natural frequency to the fiber angle increase diminishes as the fiber angle increases.

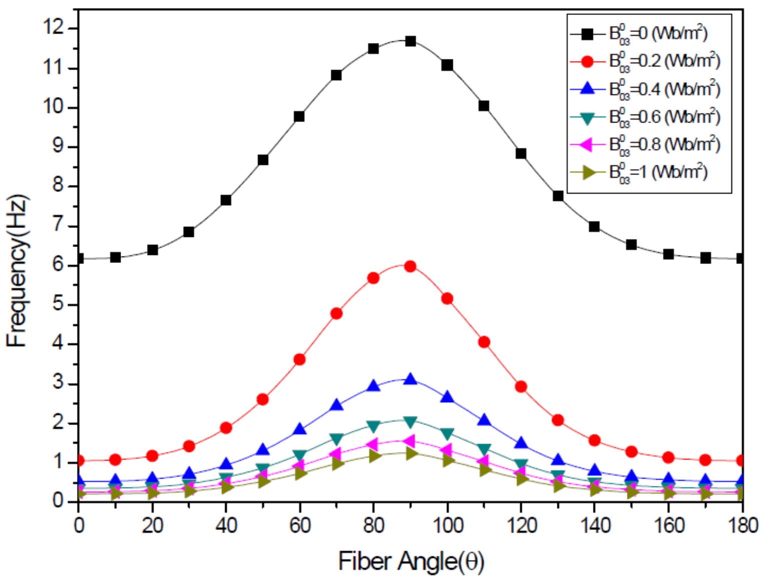

Fig. 2 Variation in the natural frequency with fiber angle
for different B_{03}^{0}

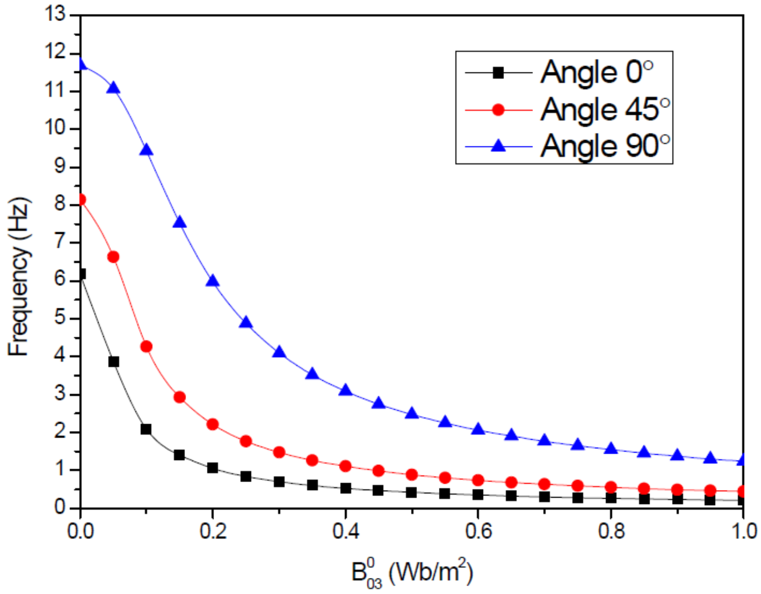

Fig. 3 Variation in the natural frequency with B^0_{03}
for three different fiber angles

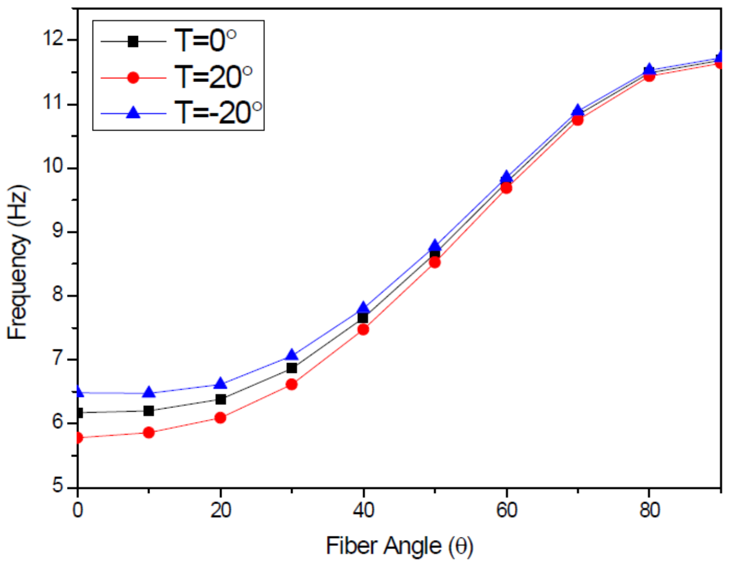

Fig. 4 Variation in the natural frequency with fiber angle
for three different temperature gradients

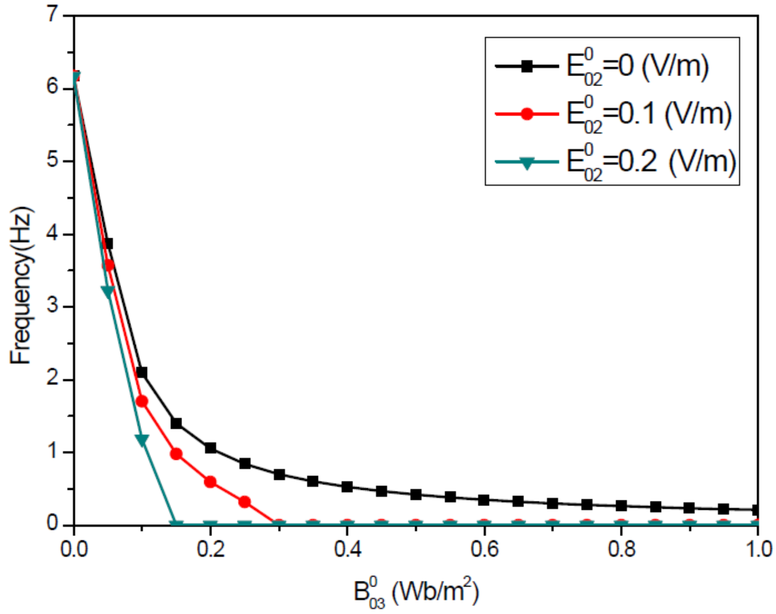

Fig. 5 Variation in the natural frequency with B_{03}^{0}
for three different electric fields

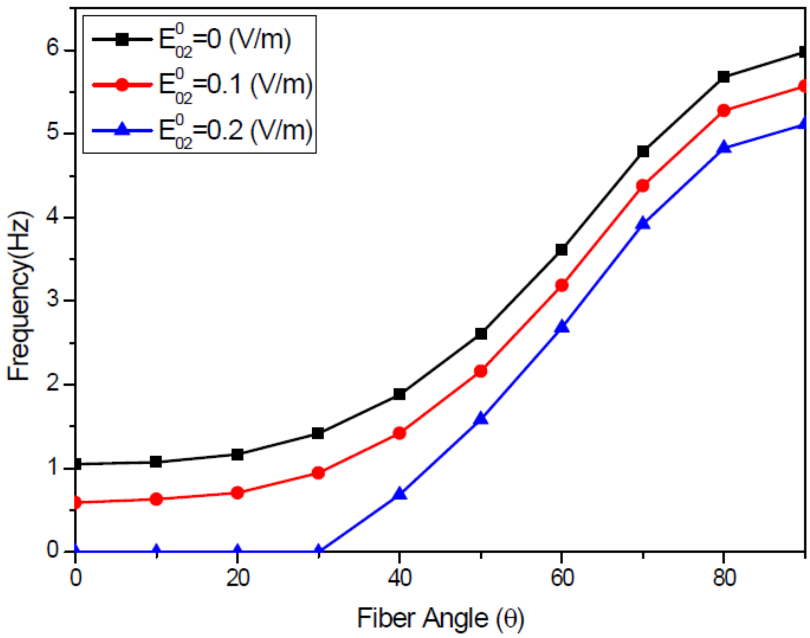

Fig. 6 Variation in the natural frequency with fiber angle
for three different electric fields

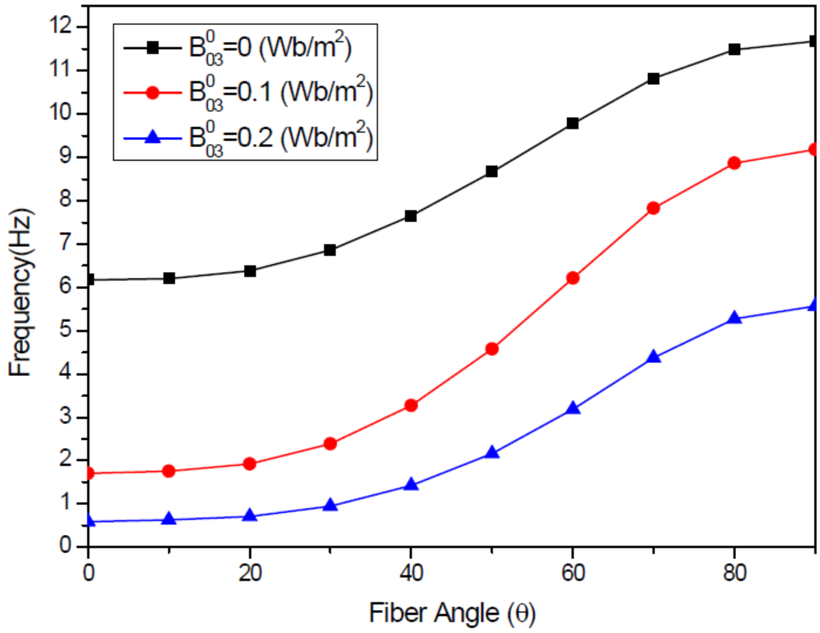

Fig. 7 Variation in the natural frequency with fiber angle for different B_{03}^{0}

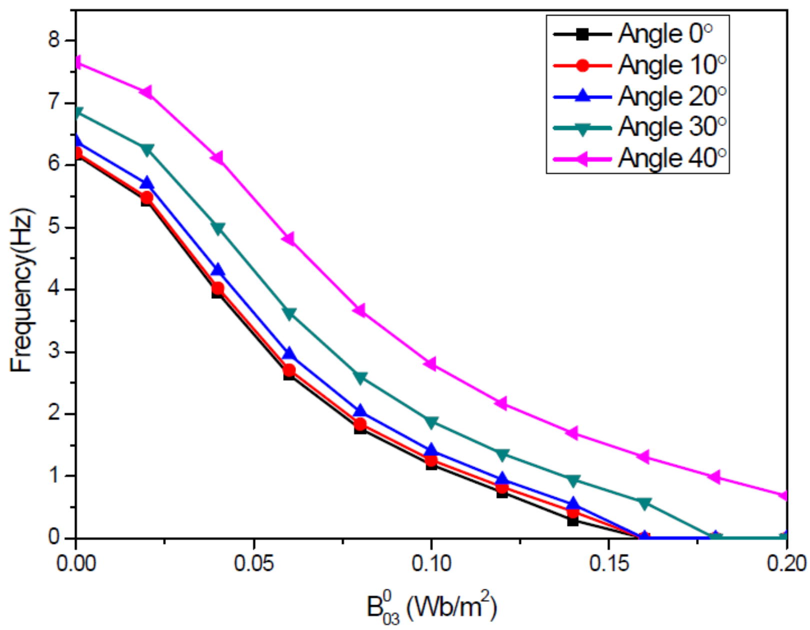

Fig. 8 Variation in the natural frequency with B_{03}^{0} for different fiber angles

4. CONCLUSION

In this study, dynamic characteristics of composite thin-walled beam structures subjected to interactive elastic, thermal, electromagnetic fields is investigated. In order to secure the reliability of analysis results, the effect of shear strain and the rotary inertia that constitutes a non-classical effect is considered. Extended Galerkin method is adopted to obtain the discretized equations of motion. Variations of dynamic characteristics of composite thin-walled beam subjected to a combined electromagnetic and thermal field are investigated.

ACKNOWLEDGEMENT

This work is supported by the Basic Science Research Program through the National Research Foundation of Korea (NRF) funded by the Ministry of Education, Science and Technology (No.2013-053626).

REFERENCES

Park, S.Y. Song, O. S. (2014). “Piezoelectric Control of Multi-functional Composite Shells Subjected to an Electromagnetic Field”, ACEM’14 Conference

Kim, S.K., Lee, K.W., Moon, J.K., Choi, J.W., Kim, Y.J., Park, S.Y. Song, O. S. (2011), “Dynamic characteristics of composite plate subjected to electromagnetic and thermal field,” KSNVE, **22**(8), 536-546.

Song, O. S., Kim, J.B., Librescu, L. (2001), “Synergistic implications of tailoring and adaptive materials technology on vibration control of anisotropic thin-walled beams”, International Journal of Engineering Science, **39**(1), 71-94.

Moon, F.C., 1984, Magneto-Solid Mechanics, John Wiley and Sons, Ithaca, New York, 288-296.

Chen, L.W., Lin, C,Y., Wang. (2002), “Dynamic stability analysis and control of a composite beam with piezoelectric layers”, Composite Structures, **56**(1), 97-109

Yoon, G. H. (2010), “Topology optimization considering the couplings of electro-fluid-thermal-compliant micro actuator,” KSME, 640-642.

Reddy J.N. (2004), *Mechanics of Laminated Composite Plates and Shells Theory and Analysis 2nd Edition*, CRC Press, New York.

L, Librescu and Song, O. S. (2006), *Thin-Walled Composite Beams: Theory and Application, Solid Mechanics and its Applications*, Volume 131, Springer

Qin, Z. and Hasanyan, D. (2011), “Fully non-linear magnetoelastic interactions of a circular cylindrical thin shell subject to electromagnetic fields,” International Journal of Non-Linear Mechanics, **46**(2), 425-435.

Tsai, Y.H. and Wu, C.P. (2008), “Dynamic responses of functionally graded magneto-electro-elastic shells with open-circuit surface conditions,” International Journal of Engineering Science, **46**(9), 843-857.